The Kinematics and Electron Cross Sections of Compton Scattering

Edwin Ng*
MIT Department of Physics
(Dated: December 7, 2011)

We scatter 661.6 keV gamma rays off NaI scintillators and use coincidence techniques to measure the energies of the scattered photons and electrons as functions of scattering angle. We observe results consistent with the kinematics of Compton scattering and obtain an estimate on the electron rest mass of $(552 \pm 15_{\text{rand.}} \pm 74_{\text{syst.}})$ keV. By measuring count rates, we also observe deviation of the differential cross section from the classical Thomson prediction in favor of the relativistic Klein-Nishina formula. Finally, attenuation of the radiation using plastics yields an estimate on the total cross section of $(0.205 \pm 0.002_{\text{rand.}} \pm 0.032_{\text{syst.}})$ b, also in preference of the relativistic prediction.

I. THEORY OF THE EXPERIMENT

I.1. Compton Scattering

Classically, electromagnetic radiation interacts with charges by Thomson scattering, via dipole radiation. However, at energies $\sim$ 1MeV, we instead observe Compton scattering, a relativistic interaction first discovered in the 1920s by Arthur Compton as a wavelength shift ("Compton effect") in scattered x-rays.[1]

From early quantum theory, we can view light as a "photon" with both momentum and energy. Suppose a photon of energy E scatters off a free electron at rest. Then viewing the photon as an ultrarelativistic particle with momentum $p = E/c$, the scattered energy E' follows

$$\frac{1}{E'} - \frac{1}{E} = \frac{1}{mc^2}(1 - \cos\theta) \tag{1}$$

where θ is the scattering angle and mc^2 is the electron rest mass energy. As a result of energy conservation, the scattered kinetic energy E_e of the electron is $E - E'$, so

$$\frac{1}{E_e} - \frac{1}{E} = \frac{mc^2}{E^2}\frac{1}{1 - \cos\theta} \tag{2}$$

Thus, from either Equations 1 and 2, measurements of E_e and E' due to Compton scattering of a known incident source can be fit to a linear relationship, to yield mc^2.[2]

I.2. Electron Cross Section

In a typical scattering experiment, an incident flux I_0 of photons strike a target volume containing n electrons, and the scattered photon is picked up by a detector subtending a solid angle $\mathrm{d}\Omega$. Suppose events occur at this detector with rate N. Then the "effective scattering area" $\mathrm{d}\sigma$ of each electron is related by $I_0 n\,\mathrm{d}\sigma = N$, so

$$\frac{\mathrm{d}\sigma}{\mathrm{d}\Omega} = \frac{N}{I_0 n\,\mathrm{d}\Omega} \propto N \tag{3}$$

For small $\mathrm{d}\Omega$, the variation of $\mathrm{d}\sigma/\mathrm{d}\Omega$ as a function of θ is defined to be the *differential cross section*.[3]

Depending on our theoretical model of the scattering process, predictions of the differential cross section can be radically different. In Thomson scattering, a simple analysis of dipole radiation gives

$$\frac{\mathrm{d}\sigma}{\mathrm{d}\Omega} = r_0^2\left(\frac{1 + \cos^2\theta}{2}\right) \tag{4}$$

where r_0 is the classical electron radius. However, in order to account for the quantum and relativistic behavior of higher energy photons, we require the Klein-Nishina formula[4] derived in quantum electrodynamics:

$$\frac{\mathrm{d}\sigma}{\mathrm{d}\Omega} = r_0^2\left(\frac{1 + \cos^2\theta}{2}\right)\Gamma(\gamma) \tag{5}$$

where we define $\gamma = E/mc^2$, and $\Gamma(\gamma)$ to be

$$\left[\frac{1}{1 + \gamma(1 - \cos\theta)}\right]^2\left[1 + \frac{\gamma^2(1 - \cos\theta)^2}{(1 + \cos^2\theta)\big(1 + \gamma(1 - \cos\theta)\big)}\right]$$

Note that at low energies, as $\gamma \to 0$, $\Gamma \to 1$ and agrees Equation 4. In this experiment, we will compare our results against these two predictions.

Finally, the *total cross section* σ is the "effective area" of the electron when scattering into *all* angles and is therefore defined as the integral of $\mathrm{d}\sigma/\mathrm{d}\Omega$.

Alternatively, suppose we send a beam of photons with flux I_0 into a material, with the primary interaction being Compton scattering off electrons. Then if there are n_e electrons per unit volume of material, the linear attenuation μ of the beam flux relates to σ by $\mu = \sigma n_e$, and the attenuated flux is $I(x) = I_0 e^{-\mu x}$ where x is the depth of the material.[1] Now, $I \propto N$, the count rate of a detector measuring the attenuated beam. Letting N_0 be the count rate corresponding to I_0, we have

$$\log\frac{N_0}{N(x)} = -\mu x \tag{6}$$

With μ, we can obtain $\sigma = \mu/n_e$. We will use this equivalent formulation to measure the total cross section of the electron due to Compton scattering, and compare the result against the integrated predictions of Thomson and Klein-Nishina.

* ngedwin@mit.edu

II. EXPERIMENTAL SETUP

II.1. Apparatus and Coincidence

The setup consists of a ^{137}Cs 661.6 keV ($\approx$ 100 µCi) gamma source in a height-adjustable lead howitzer and two NaI detectors, labeled "target" and "scattering", for picking up recoiled electrons and scattered photons, respectively. See Figure 1 below for the geometry. The following discussion draws from [2].

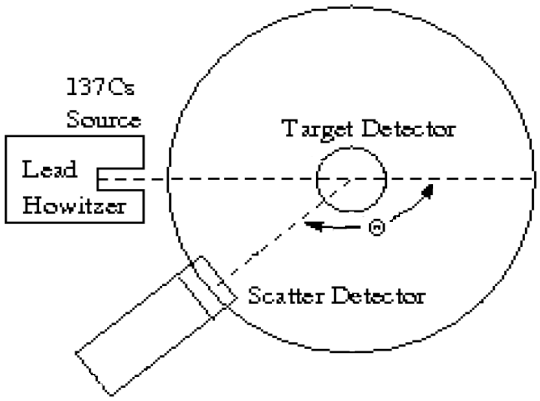

FIG. 1. A top-down view of the table top setup. The scattering detector (horizontal) is free to rotate by θ, while the recoil detector (vertical) is fixed. The circular table also has angles marked along the edge. Adapted from [2].

We set the howitzer height to align with the target crystal. The distance from the source to the target is about 25cm; to the scattering is another 25cm. The scattering detector face subtends about 8°. We use lead blocks to minimize noise from multiple-scatterings.

The NaI detectors are Canberra Model 802, $2'' \times 2''$ NaI scintillators, attached to photomultiplier tubes biased by Canberra HV power supplies (3105 for target; 3002D for scattering) at approximately 1000V. The signal is then passed through a Canberrra preamplifier (2007, attached to preamp for target; 805, separated for scattering), and into Ortec amplifiers. Gain settings changed from day to day, but settings of rough gain 4 and fine gain ≈ 7 are typical. The output of the signal chain is captured by two multichannel analyzers (MCAs), one for each detector, which bin the voltage signals into 2048 channels each.

A key aspect of this lab is using coincidence techniques to select out scattering events at angles of interest. The incident photons interact with the target detector by both photoelectric absorption and Compton scattering. The former creates a photopeak, but in the latter, the energy of the "recoiled" electron depends on the scattering angle, so it can lie anywhere along the "Compton continuum". (See Figure 2.) On coincidence, the MCAs only record signals when both detectors register simultaneously (within $\sim$ 1µs), so we "filter" the the recoil spectrum, selecting for the part of the continuum corresponding to a θ-scattering. This allows us to discern the E_e and E' peaks.

To implement coincidence, we feed the output of the amplifier through Ortec inverters and into Canberra Model 2126 constant fraction discriminators. Typical settings we use for the threshold are 0.1. The output of the discriminators are sent through an Ortec 418A coincidence. The output is then fed into a Ortec gate and delay generator, outputting TTL pulses at 10 V, width 4 µs. These pulses are plugged into the gate inputs on the MCAs, which use the pulses to gate the signals on coincidence mode.

One important check on the signal chain is of the gate and delay generator, to ensure the peaks of both coincident signals fall under the gate. We note that, on occasion, one of our two signals would appear outside the gate. The effect is erratic and hard to capture with a scope; it also seems to switch detectors across lab sessions. Its effect on our data is unknown, but we suspect it can affect the relative count rates of the two detectors.

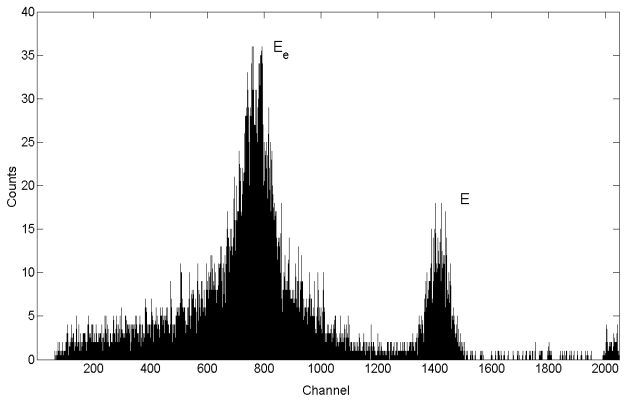

FIG. 2. A recoil spectrum at 45°. Because of false coincidences, we see a suppressed photopeak at 661.6 keV and some of the Compton continuum/noise. Note the distinguished recoil peak, due to coincidence.

II.2. Calibration

To determine the relation between the channel numbers and energy, we calibrate both signal chains each lab session with ^{133}Ba and ^{22}Na, running the MCAs with coincidence off and the calibration source placed halfway between the two detectors for $\sim$ 300 s. We use the 81 keV and 356 keV lines for ^{133}Ba and 511 keV for ^{22}Na.

We find the calibration peaks using the same fit procedure described in Section III.1. We use Gaussian/linear for ^{133}Ba and Gaussian/exponential for ^{22}Na. To relate energy T and channel n, we use the linear model $E = \alpha n + \varepsilon$, where α is the energy per channel and ε is the energy offset at zero.

As an example, for 11/09, $\alpha = (0.460 \pm 0.002)$ keV/ch and $\varepsilon = (-14.1 \pm 1.7)$ keV for scattering and $\alpha = (0.473 \pm 0.002)$ keV/ch and $\varepsilon = (-10.8 \pm 1.7)$ keV for recoil.

N.B.: Interestingly, ignoring ε and redoing the analysis in Sections III.1/IV.1 brings $E' + E_e \approx 670$ keV for most angles. However, we can not justify the approach, and it also exaggerates the mc^2 difference between recoil and scattering estimates (e.g., 360 keV vs. 620 keV).

III. PROCEDURE AND DATA

III.1. Angle Measurements

With coincidence on, we collect MCA acquisitions for both detectors at various angles. On 11/09, we took data for 45°, 90°, 120°, 135°, and 150°, with a 30° overnight run immediately following. We also took 60° data twice, once on 11/07 and once on 11/14. Acquisition times were $\sim 1000\,\mathrm{s}$, with the exception of the overnight run, which lasted $\sim 55000\,\mathrm{s}$ (about 1000 s dead time). Adjustments are made for each angle in order to reposition the lead blocks and align the center of the detector with the angle of interest, but otherwise, the setup remains constant.

Once MCA spectra are obtained, the next step is to fit the data to extract the location of peaks. We capture the peak behavior by considering a Gaussian, superimposed on a background following either a linear or exponential decay model. We use the linear background for $\theta < 90°$, and the exponential otherwise. The functional forms are

$$y = \frac{A}{\sqrt{2\pi\sigma^2}} \exp\left[-\frac{(x-n)^2}{2\sigma^2}\right] + Bx + C \tag{7}$$

$$y = \frac{A}{\sqrt{2\pi\sigma^2}} \exp\left[-\frac{(x-n)^2}{2\sigma^2}\right] + Be^{-x/C} \tag{8}$$

In particular, we are interested in the photopeak of the scattered spectrum, and the recoil peak of the target spectrum. We choose our region of interest (ROI) around the peak to be about 2σ in each direction, and we examine the residues of each plot to eliminate systematic shifts of the peak. Using the amplification ratios and offsets from the appropriate calibration, we find the peak energies E' and E_e, which we summarize in Table I.

TABLE I. MCA peak energies by angle and their sum. Note that two measurements were made at 60°, so its errors include systematic disagreements.

θ	E' (keV)	E_e (keV)	E (keV)
30	479.7 ± 3.2	116.0 ± 2.3	595.7 ± 3.9
45	465.3 ± 3.2	179.9 ± 2.1	645.2 ± 3.8
60	394.7 ± 16.	243.1 ± 3.0	637.8 ± 16.
90	295.5 ± 2.6	352.8 ± 2.6	648.3 ± 3.7
120	229.7 ± 2.2	414.5 ± 2.8	644.2 ± 3.6
135	211.6 ± 2.1	431.8 ± 2.9	643.4 ± 3.6
150	193.7 ± 2.1	448.4 ± 2.9	642.1 ± 3.6

Also of interest in the angle measurements will be the count rates at the scattering detector, in determining the differential cross section. Here, we simply extract the number of counts over all channels and divide by the live time of acquisition. Hence, for N_0 total counts, $N_0 = M/T \pm \sqrt{N_0}/T$. We also do not consider the 30° measurement for count rate purposes, because examination of the overnight spectrum reveals a $\sim 1000\,\mathrm{s}$ discrepancy between the live times of the two detectors, suggesting the scattering detector was possibly overwhelmed by its proximity to the beam.

However, the count rates are not the whole story—we have to correct for detector efficiencies. Using [5], we determine the energy-dependent counting efficiencies η_0 and peak-to-total ratios $\eta_{\text{P-T}}$. Suppose the scattering detector is being irradiated with only E' gamma rays. Then η_0 is the probability the gamma ray will interact with the detector, while $\eta_{\text{P-T}}$ is the probability that, given it interacts, it does so via photoelectric effect (as opposed to another Compton scattering). The corrected count rate N' would therefore be $N' = N/(\eta_0\eta_{\text{P-T}})$. We use the theoretical values of E' in reading off η values. The results are summarized in Table II below.

TABLE II. Count rates and efficiency-corrected count rates.

θ	N (cps)	$\eta_{\text{P-T}}$	η_0	N' (cps)
45	9.55 ± 0.08	0.66	0.83	17.43 ± 0.14
60	8.68 ± 0.08	0.72	0.89	13.55 ± 0.12
90	6.32 ± 0.07	0.85	0.96	7.75 ± 0.08
120	5.47 ± 0.07	0.95	0.99	5.82 ± 0.07
135	6.06 ± 0.08	0.97	1.00	6.25 ± 0.09
150	8.92 ± 0.10	1.00	1.00	8.92 ± 0.10

III.2. Total Cross Section Measurements

As suggested by the alternate definition of total cross section in Section I.2, we send the beam through various materials to determine the attenuation μ, from which we obtain σ. We use three plastic materials, polycarbonate (PC), polypropylene (PP), and polyvinyltoluene (PVT), in the form of blocks (four each, except PVT, with five) that we place in front of the howitzer. The block thicknesses are 1.20 cm, 2.45 cm, and 2.50 cm, respectively.

We remove the target detector and place the scattering detector at $\theta = 0$ to intercept the beam. First, we measure the unattenuated count rate N_0, and then for each material, we place successive blocks in front of the howitzer for each measurement. We acquire for 100 s.

We fit the resulting peaks using the same techniques as in Section III.1, using the Gaussian/exponential model, Equation 8. We then subtract out $Be^{-x/C}$ (the background model) from the ROI, and sum the remaining counts. To obtain N, we then divide by the time of acquisition, and compute the error as before.

Finally, the trend of $\log N(x)/N_0$ against x, where x is the total thickness used, is fit using Equation 6, and the value of μ extracted. The number density of electrons n_e is determined by $n_e = \mathcal{N}\rho\langle Z/A\rangle$, where $\mathcal{N}$ is Avogadro's number, ρ is the density, and $\langle Z/A\rangle$ is the mean charge/mass number ratio. The results, along with $\sigma = \mu/n_e$ for each material, are given in Table III.

TABLE III. Attenuations and cross sections for plastics.

Material	μ (10^{-2}/cm)	χ^2_ν	n_e (cm^{-3})	σ (b)
PC	9.8 ± 0.2	1.0	5.13×10^{23}	0.191 ± 0.005
PP	7.9 ± 0.1	0.3	4.50×10^{23}	0.175 ± 0.003
PVT	8.0 ± 0.1	1.4	3.35×10^{23}	0.239 ± 0.003

IV. ANALYSIS OF DATA

IV.1. Compton Kinematics

Using the reduced data in Table I, we can fit the values of E' and E_e against θ according to Equations 1 and 2. The linear fit for the scattering is shown in Figure 3.

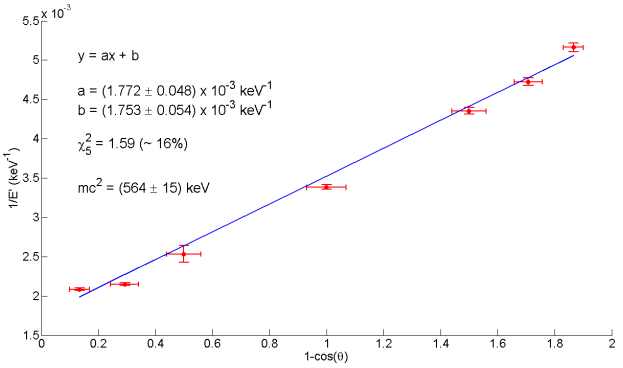

FIG. 3. Linear fit of $1/E'$ vs $1-\cos\theta$ according to Eq. 1.

In our setup, we align the center of the detector on the angle θ of interest. However, as we know from the theory of differential cross section, the strongest signal at that position does not come from photons scattered through θ, but from an angle slightly to the left or right, depending on the gradient of $\mathrm{d}\sigma/\mathrm{d}\Omega$. Hence, there is a *systematic error* on the angle determination, which depends on the differential cross section in addition to the geometry of the setup. For a conservative estimate on this error, we use its upper bound due to the detector width. Since the scattering detector subtends an angle 8°, we bound this source of systematic error by ±4°.

The result of the fit for the scattering detector yields an estimate on $mc^2 = (564 \pm 15)\,\mathrm{keV}$, with a $\chi^2_5 = 1.59$ (16%). The value of χ^2 is rather high, and this compounds with the fact that our estimate on the error on θ is high to begin with. Nevertheless, the dependence of the energy on angle is manifestly Compton.

We do a similar fit for the recoil detector using again the values in Table I. On this one, we fit $1/E_e$ against $(1-\cos\theta)^{-1}$, as dictated by Equation 2. The resulting fit to $y = ax + b$ yields $a = (1.14 \pm 0.12) \times 10^{-3}\,\mathrm{keV}^{-1}$ and $b = (1.65 \pm 0.09) \times 10^{-3}\,\mathrm{keV}^{-1}$, so that $mc^2 = (418 \pm 50)$. We also get $\chi^2_5 = 0.87$ (50%).

Taking these two results and averaging, we find our best estimate of $mc^2 = (552 \pm 15)\,\mathrm{keV}$ with a systematic error given by half the difference, which is $\pm 74\,\mathrm{keV}$.

IV.2. Differential Cross Section

We plot the corrected count rates N' in Table II against θ according to Equation 3 to obtain the differential cross section profile. To sidestep possible errors that come out of trying to estimate the value of the experimental constant $I_0 n$, we multiply it into the overall scale on Equations 4 and 5 when doing our fit. The shape of the curve itself should not change, and we can check the scale afterwards to ensure it is sensible. The fits for Thomson (Eq. 4) and Klein-Nishina (Eq. 5) are shown in Figure 4.

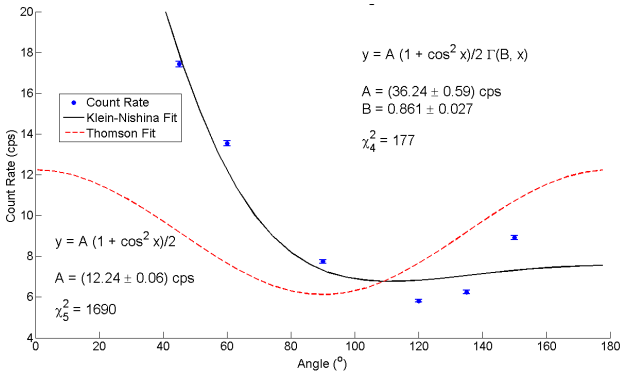

FIG. 4. Fit of $N' = I_0 n(\mathrm{d}\sigma/\mathrm{d}\Omega)$ against θ. Note that for reasons given in Section III.1, 30° is omitted.

Although neither fit is satisfying, we see that the Thomson prediction is overwhelmingly bad, as compared to the Klein-Nishina formula: the value of reduced χ^2 are 1690 and 177, respectively. It is clear the error estimates on the data points are heavily underestimated. There are certainly systematic errors on the angles, in addition to difficulty in correcting for the detector efficiencies, which are not very well documented (see for example [5]).

What is more encouraging is the overall scale factor on the Klein-Nishina fit. The algorithm gives $A = (36.24 \pm 0.59)\,\mathrm{cps}$. Since $A = I_0 n r_0^2\,\mathrm{d}\Omega$ where r_0 is the classical electron radius, we can perform a useful, independent order-of-magnitude calculation, due to KG.

The ^{137}Cs source is rated at 500 µCi in 1991. Since ^{137}Cs has a half-life of about 30 yr, we expect the radioactivity to be about 300 µCi, which translates to a flux of $I_0 \simeq 1000\,\mathrm{s}^{-1}/\mathrm{cm}^{-2}$ (using 30 cm as the target to detector radius—see Section II.1). In the volume of the NaI crystal (face diameter and height 5 cm), $n \simeq 10^{26}$. Lastly, we find $\mathrm{d}\Omega \simeq 0.01\,\mathrm{sr}$. Putting this all together, we estimate $r_0 \simeq 2 \times 10^{-13}\,\mathrm{cm}$ which, compared to the correct value of $2.87 \times 10^{-13}\,\mathrm{cm}$ is remarkable, especially since the Thomson prediction is off by a factor of two.

IV.3. Total Cross Section

From the values presented in Table III, we can work out an average value for the total cross section. This yields a best estimate of $\sigma = (2.05 \pm 0.02) \times 10^{-25}\mathrm{cm}^2$, or (0.205 ± 0.002)b. We take the systematic error to be half the difference, or ±0.032b.

In general the reduced χ^2 values on the fits for Equation 6 are good. However, we note that while Equation 6 has zero slope intercept, the fits that resulted had small but not completely negligible intercepts, on the order of 0.02 on the largest one, corresponding to a disagreement on N_0 of 2%.

V. CONCLUSIONS

In general, measurements of the scattered energies of both photons and electrons as functions of scattering angle show agreement with the predictions of Compton kinematics. From this, we are able to derive an estimate on the electron rest mass of $(552 \pm 15_{\text{rand.}} \pm 74_{\text{syst.}})$ keV, which is about a 2% error (though with 14% uncertainty).

Furthermore, measuring count rate as a function of scattering angle yielded the differential cross section profile of the electron, which agrees at least qualitatively with the Klein-Nishina formula from quantum electrodynamics, and deviates significantly from the classical Thomson prediction. The data gives a correct order of magnitude estimate for the classical electron radius, at 2×10^{-13} cm.

Finally, we measure the total electron cross section to be $(0.205 \pm 0.002_{\text{rand.}} \pm 0.032_{\text{syst.}})$ b. The theoretical value due to the Klien-Nishina formula is 0.257 b, while the Thomson prediction is 0.665 b. Our result agrees with the relativistic value to about 1.5σ, and shows a clear preference for the correctness of the quantum theory of electrodynamics.

[1] R. Eisberg and R. Resnick, *Quantum Physics of Atoms, Molecules, Solids, Nuclei, and Particles*, 2nd ed. (John Wiley & Sons, 1985).
[2] M.I.T. Junior Lab Staff, "Compton Scattering," (2011).
[3] D. J. Griffiths, *Introduction to Quantum Mechanics*, 2nd ed. (Pearson Education, Inc., 2005).
[4] A. Melissinos, *Experiments in Modern Physics* (Academic Press, 1966).
[5] Saint-Gobain Crystals, "Efficiency calculations for selected scintillators," (2008).

ACKNOWLEDGMENTS

EN gratefully acknowledges his lab partner, Kevin Galiano, and the Junior Lab staff for their assistance in understanding the theory behind the design and analysis of this experiment.